Overexpression of SOD-2 reduces hippocampal superoxide and prevents memory deficits in a mouse model of Alzheimer's disease

Cynthia A. Massaad[a], Taneasha M. Washington[a], Robia G. Pautler[a,1] and Eric Klann[b,1,2]

[a]Department of Molecular Physiology and Biophysics, Baylor College of Medicine, Houston, TX 77030; and [b]Center for Neural Science, New York University, New York, NY 10003

Communicated by Susumu Tonegawa, Massachusetts Institute of Technology, Cambridge, MA, April 15, 2009 (received for review February 12, 2009)

Alzheimer's disease (AD) is a neurodegenerative disease characterized by impaired cognitive function and the deposition of extracellular amyloid plaques and intracellular tangles. Although the proximal cause of AD is not well understood, it is clear that amyloid-β (Aβ) plays a critical role in AD pathology. Recent studies also implicate mitochondrial abnormalities in AD. We investigated this idea by crossing mice that overexpress mitochondrial superoxide dismutase (SOD-2) with the Tg2576 mouse model of AD that overexpresses the human amyloid precursor protein carrying the Swedish mutation (K670N:M671L). We found that overexpression of SOD-2 decreased hippocampal superoxide, prevented AD-related learning and memory deficits, and reduced Aβ plaques. Interestingly, SOD-2 overexpression did not affect the absolute levels of $A\beta_{1-40}$ and $A\beta_{1-42}$, but did significantly reduce the $A\beta_{1-42}$ to $A\beta_{1-40}$ ratio, thereby shifting the balance toward a less amyloidogenic Aβ composition. These findings directly link mitochondrial superoxide to AD pathology and demonstrate the beneficial effects of a mitochondrial anti-oxidant enzyme, hence offering significant therapeutic implications for AD.

antioxidant | dementia | mitochondria | oxidative stress | reactive oxygen species

Alzheimer's disease (AD) is a progressive neurodegenerative disease characterized by the neuropathological deposition of extracellular amyloid plaques and intracellular neurofibrillary tangles, as well as impairment of cognitive functions (1). Although the potential neurotoxic effect of amyloid-β (Aβ) has been long established (2), its specific role in the cascade of events leading to memory impairments is unknown. Several reports propose a link between Aβ and oxidative stress to explain the downstream cognitive deficits in AD. Specifically, it has been shown that Aβ promotes oxidation in several model systems (3, 4) and conversely, pro-oxidants increase the production of Aβ (5). Thus, reducing oxidative stress through antioxidant supplementation has received considerable attention as a therapy for AD. Unfortunately, antioxidant trials have produced conflicting results (6, 7), perhaps because dietary antioxidant supplementation does not afford the specificity of targeted pharmacological therapy. There are several enzymatic sources of reactive oxygen species (ROS) in mammalian neurons, including peroxidases, NADPH oxidase, and xanthine oxidase, as well as organelles containing electron transport systems such as lysosomes and mitochondria. Investigating one potential source of ROS would provide a more specific therapeutic target for AD. We chose mitochondria because several reports have suggested the involvement of mitochondrial abnormalities and oxidative damage in the etiology of AD (8, 9). For example, soluble Aβ species have been linked to an increased hydrogen peroxide and decreased cytochrome C oxidase activity in the Tg2576 mouse model of AD (10). Additionally, both amyloid precursor protein (APP) and Aβ have been shown to enter the mitochondria: APP contributes to energy processing dysfunction (11) and Aβ causes a signaling amplification that inactivates superoxide dismutase (SOD-2) and generates additional free radicals (12). Moreover, AD model mice crossed with SOD-2 heterozygous knockout mice exhibited increased plaque burden in their brains (13). Finally, a global increase in SOD-2 has been observed in AD patients, presumably as a compensatory mechanism in response to AD-associated oxidative stress (14). This increase, however, is less pronounced in hippocampal area CA1 (14), which is required for memory formation and suffers the most neuronal degeneration during AD (15).

We hypothesized that SOD-2 overexpression could prevent AD-related cellular pathology and memory impairments in the Tg2576 mouse model of AD. To test this hypothesis we assessed the cognitive function of Tg2576 mice overexpressing SOD-2 at ages ranging from 4 to 16 months. Histological assessment of superoxide levels and plaque deposition, and levels of soluble and fibrillar β-amyloid species also were determined. Our findings suggest that the impact of mitochondrial ROS on Aβ composition may be a key event in the initiation of AD-related cellular pathology and memory dysfunction.

Results

We first measured the levels of SOD-2 in the SOD-2 overexpressing mice and found increased expression compared with wild-type (WT) and Tg2576 mice (Fig. 1*A*). We also confirmed increased expression of APP in the Tg2576 mice (Fig. 1*A*). We then measured the levels of superoxide in the hippocampus by using dihydroethidium (DHE) staining (16). We found that Tg2576 mice exhibited higher levels of hippocampal superoxide compared with WT littermates (Fig. 1 *B* and *C*). Interestingly, superoxide levels also progressively increased with age, with the >12-month-old mice exhibiting a higher level of superoxide than the 8-month-old mice. This is in agreement with previous reports in the literature showing an age-dependent increase in hippocampal superoxide that is returned to normal by SOD-2 overexpression (17). In Tg2576 mice, there is a further increase in superoxide that also was reduced with SOD-2 overexpression (Fig. 1 *B* and *C*). These data confirm the functionality of the overexpressed SOD-2 in the double transgenic mice.

We then subjected the mice to a battery of behavioral tests to evaluate the effects of the transgenes on locomotor activity (Fig. S1), motor coordination and balance (Fig. S2), and sensorimotor gating (Fig. S3). Regardless of genotype or age, all mice scored similar to controls in all tests. One interesting observation was that 12-month-old Tg2576 mice exhibited a trend toward in-

Author contributions: C.A.M., R.G.P., and E.K. designed research; C.A.M. and T.M.W. performed research; C.A.M. analyzed data; and C.A.M., R.G.P., and E.K. wrote the paper.

The authors declare no conflict of interest.

[1]R.G.P. and E.K. contributed equally to this work.

[2]To whom correspondence should be sent at: Center for Neural Science, New York University, 4 Washington Place, Room 809, New York, NY 10003. E-mail: eklann@cns.nyu.edu.

This article contains supporting information online at www.pnas.org/cgi/content/full/0902714106/DCSupplemental.

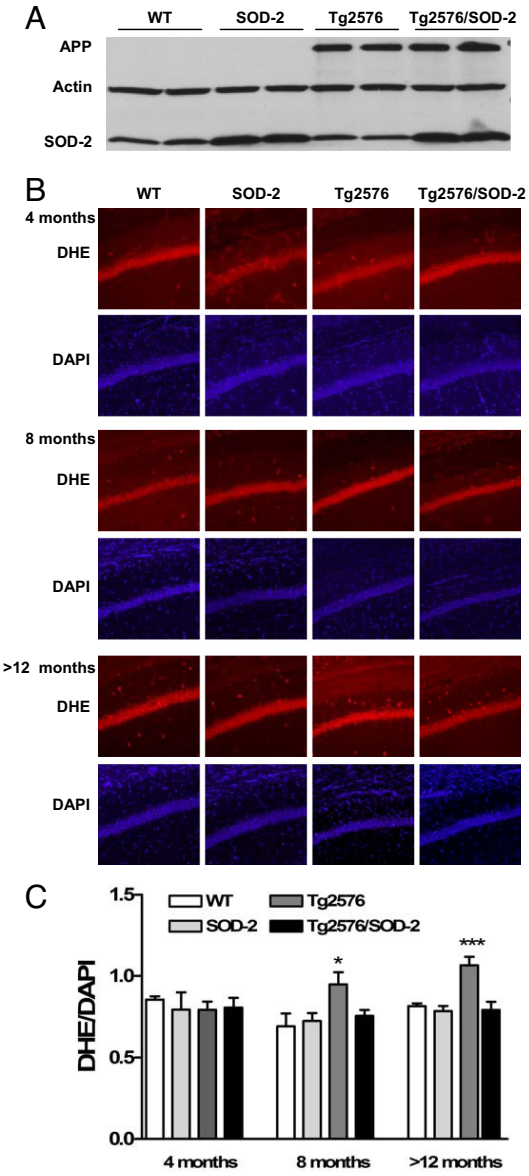

Fig. 1. SOD-2 overexpression prevents age-related increases in superoxide in Tg2576 mice. (*A*) Representative Western blot of APP and SOD-2 from brain homogenates of >12-months-old WT, SOD-2, Tg2576, and Tg2576/SOD-2 mice. (*B*) Coronal sections through area CA1 of the hippocampus showing genotype differences in ethidium fluorescence. (*C*) DHE fluorescence was measured with ImageJ software by using 1/4-inch squares throughout the soma of CA1 pyramidal cells, and then normalized to DAPI intensity. At least 10 sections per mouse were analyzed. Significance was assessed by one-way ANOVA with Tukey's post test. For WT, SOD-2, Tg2576, and Tg2576/SOD-2 mice, respectively, $n = 2, 2, 2$, and 4 at 4 months of age; $n = 5, 5, 5$, and 5 at 8 months of age; and $n = 10, 8, 9$, and 9 at >12 months of age. *, $P < 0.05$; ***, $P < 0.001$.

creased locomotion that was blocked by SOD-2 overexpression (Fig. S1 *C* and *F*). Although this trend was not significant, this type of hyperactivity has been observed in several lines of APP mutant mice (18–21). The observation that SOD-2 overexpression prevented the hyperactivity displayed by the Tg2576 mice is consistent with the notion that SOD-2 blocks adverse effects associated with Aβ accumulation.

Tg2576 mice exhibit both associative and spatial memory deficits as they age (22, 23). These deficits appear starting at 6 months of age, in correlation with increased Aβ species (22). We also observed that the Tg2576 mice have severe associative learning and memory impairments at 8 and >12 months of age, as their freezing behavior was significantly decreased compared with WT littermates when tested either 1–2 h (short-term memory) or 24–25 h (long-term memory) after training (Fig. 2 *A–F*). The Tg2576 mice exhibited freezing during the training session that was indistinguishable from that of their wild-type littermates (Fig. S4), indicating that the Tg2576 mice had normal shock sensitivity. In contrast to Tg2576 mice, the Tg2576/SOD-2 double transgenic mice at 8 and >12 months of age exhibited behavior similar to WT mice tested either 1–2 or 24–25 h after training (Fig. 2 *A–F*). Four-month-old mice performed similar to WT littermates. We also determined whether the overexpression of SOD-2 could prevent spatial memory impairments exhibited by the Tg2576 mice (22). Eight- and >12-month-old Tg2576 mice exhibited a severe deficit in spatial memory during the probe test in the Morris water maze (Fig. 2 *J–O*). Tg2576 mice overexpressing SOD-2 had a significantly better ability to associate spatial cues with the platform location. As a result, they scored similar to their WT littermate controls on the probe test (Fig. 2 *J–O*). Regardless of the genotype, mice did not differ with respect to swim speed, distance traveled, or ability to locate a visible platform (Fig. S5). Taken together, these findings demonstrate that scavenging mitochondrial superoxide by SOD-2 overexpression improves the learning and memory impairments exhibited by the Tg2576 mice.

One of the neuropathologies associated with AD is deposition of Aβ plaques in the brain (24). We measured β-amyloid plaques with thioflavin S staining and found a substantial plaque deposition in >12-month-old Tg2576 mice (cortex and hippocampus) but none in 4- and 8-month-old mice (Fig. 3), consistent with previous studies (24). Interestingly, overexpression of SOD-2 in the Tg2576 mice caused a significant reduction in plaque deposition in those >12 months old (Fig. 3), suggesting that mitochondrial superoxide plays a role in Aβ plaque formation.

Although Aβ plaques are a hallmark feature of AD, they correlate poorly with the onset of AD-related cognitive dysfunction (22, 24). Plaque reduction with SOD-2 overexpression suggests that mitochondrial superoxide may alter Aβ processing. The Aβ pool has a heterogeneous composition of multiple Aβ species in various states, most notably soluble monomers and small oligomers, and the insoluble (fibrillar) larger oligomers (reviewed in ref. 25). Therefore, we measured the levels of the two most common Aβ species, $A\beta_{1-40}$ and $A\beta_{1-42}$, in two different brain fractions. The SDS soluble fraction contains the most soluble Aβ whereas the formic acid (FA)-soluble fraction contains fibrillar Aβ (24). The ratio of $A\beta_{1-42}$ to $A\beta_{1-40}$ is a good indication of the pathological status of an individual, and has been used as a therapeutic index (26). Consistent with previous reports, we observed a significant elevation of soluble and fibrillar $A\beta_{1-40}$ and $A\beta_{1-42}$ in Tg2576 mice at 8 months of age, reaching a 10-fold increase by 12–16 months of age (Fig. 4*A*). The increase in absolute levels of all Aβ species measured was not significantly affected by overexpression of SOD-2. There was, however, a trend toward an increase in $A\beta_{1-40}$ and a decrease $A\beta_{1-42}$ in the 8-month-old Tg2576/SOD-2 mice when compared with the Tg2576 mice. This trend resulted in a significantly reduced $A\beta_{1-42}$ to $A\beta_{1-40}$ ratio (Fig. 4*B*), indicating that scavenging mitochondrial superoxide shifts the Aβ pool toward a more favorable (less amyloidogenic) composition. We observed the same significant reduction in $A\beta_{1-42}/A\beta_{1-40}$ ratio in the Tg2576/SOD-2 mice at >12 months of age despite the apparent lack of change in either Aβ species. However, it should be noted that one of the FA-soluble $A\beta_{1-42}$ values obtained from the Tg2576/SOD-2 mice in the 12-month group deviated from the mean, but it did not meet the requirements of a significant outlier ($A\beta_{1-42}$ = 1,028.413 as compared with an average of 362.68).

NEUROSCIENCE

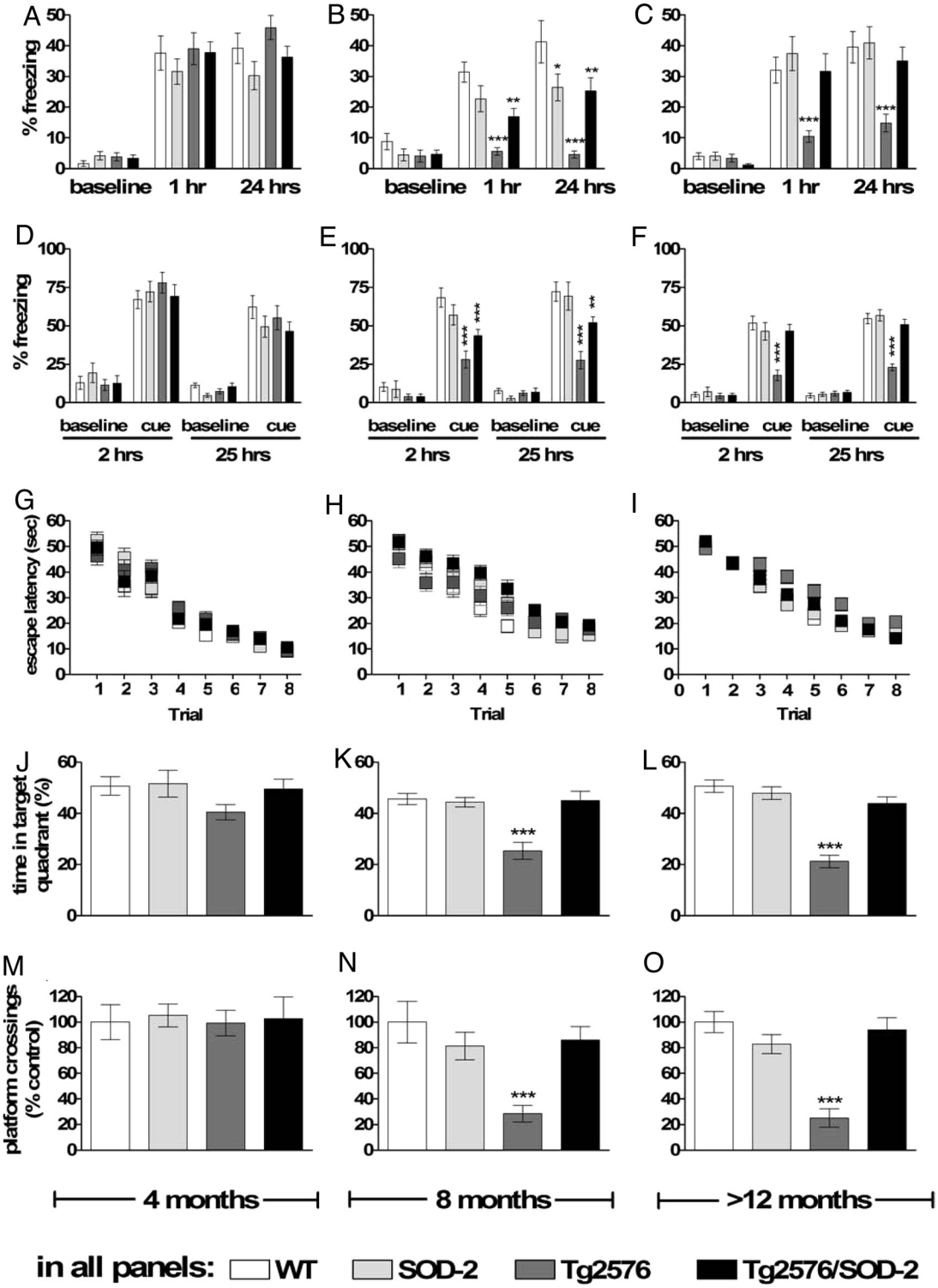

Fig. 2. SOD-2 overexpression improves both associative and spatial memory deficits displayed by Tg2576 mice. (*A–F*) Associative memory measured with fear conditioning. Graphs represent the freezing reaction of mice in response to either the context (*A–C*) or to an auditory cue (*D–F*). (G–O) Spatial memory measured with the Morris water maze. Graphs represent the latency to find the platform during training (*G–I*), and either the time spent in the target quadrant (*J–L*) or the number of target platform crossings (*M–O*) during a probe test after training. All tests were performed in 4-, 8-, and >12-month-old WT, SOD-2, Tg2576, and Tg2576/SOD-2 mice. For all tests, significance was assessed by a two-way ANOVA with Tukey's post test. Stars represent the significance of the difference between genotypes as compared with the WT within the same category. For WT, SOD-2, Tg2576, and Tg2576/SOD-2 mice, respectively, $n = 8$, 8, 8, and 8 at 4 months of age; $n = 10$, 8, 9, and 10 at 8 months of age; and $n = 18$, 16, 17, and 19 at >12 months of age. *, $P < 0.05$; **, $P < 0.01$; ***, $P < 0.001$.

This value could potentially mask a trend toward decreased $A\beta_{1-42}$ within this group. However, the ratio of this value to its corresponding $A\beta_{1-40}$ value did qualify as an outlier and was therefore not included in the analysis ($A\beta_{1-42}/A\beta_{1-40} = 3.83$ as compared to an average of 0.75). This led to a significant reduction in the $A\beta_{1-42}/A\beta_{1-40}$ ratio in the Tg2576/SOD-2 mice.

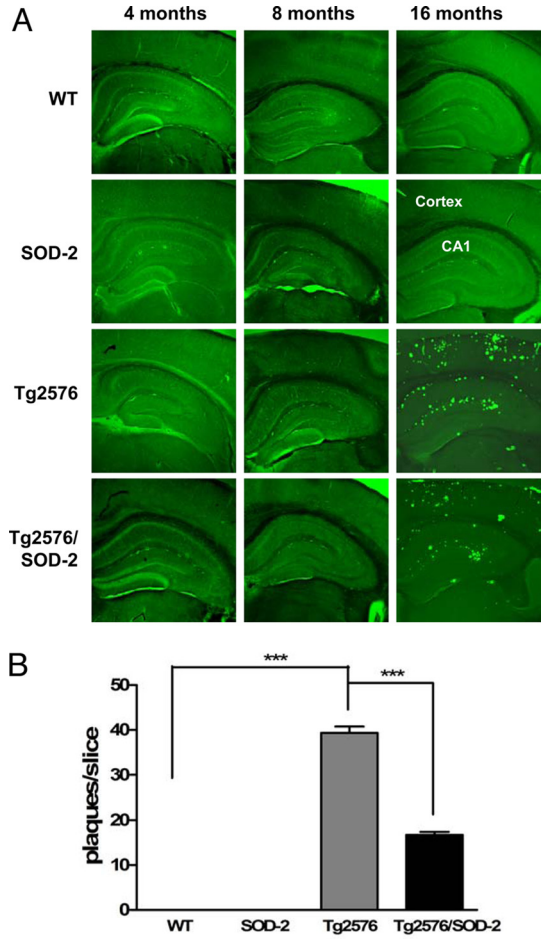

Fig. 3. SOD-2 overexpression reduces amyloid plaque formation in Tg2576 mice. (*A*) Images showing typical Thioflavin S staining of amyloid plaques in the cortex and hippocampal area CA1 of 4-, 8-, and >12-month-old WT, SOD-2, Tg2576, and Tg2576/SOD-2 mice. (*B*) Plaques were quantified by manual counting and significance was assessed by one-way ANOVA with Tukey's post test. WT, $n = 11$; SOD-2, $n = 9$; Tg2576, $n = 9$; Tg2576/SOD-2, $n = 13$; ***, $P < 0.001$.

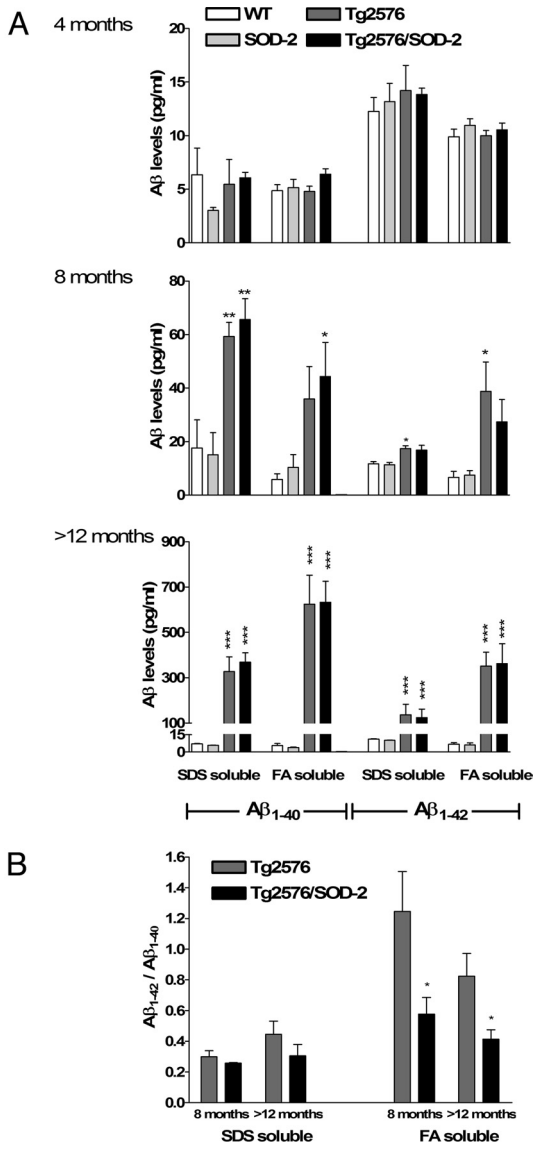

Fig. 4. SOD-2 overexpression in Tg2576 mice shifts the Aβ-species balance toward a less-amyloidogenic one without affecting absolute levels of Aβ. (*A*) Graphs represent the levels of SDS-soluble and FA-soluble $A\beta_{1-40}$ and $A\beta_{1-42}$ in 4-, 8-, and >12-month old WT, SOD-2, Tg2576, and Tg2576/SOD-2 mice. Levels were measured by sandwich ELISA and significance was assessed by one-way ANOVA with Tukey's post test. For WT, SOD-2, Tg2576, and Tg2576/SOD-2 in SDS and FA fractions respectively, $n = 2, 3, 2,$ and 7 (SDS) and 2, 3, 2, and 7 (FA) at 4 months of age; $n = 2, 3, 3,$ and 3 (SDS) and 5, 5, 5, and 5 (FA) at 8 months of age; and $n = 6, 5, 7,$ and 10 (SDS) and 12, 10, 11, and 12 (FA) at >12 months of age. *, $P < 0.05$; **, $P < 0.01$; ***, $P < 0.001$. (*B*) Graphs represent the ratio of SDS-soluble and FA-soluble $A\beta_{1-42}$ to $A\beta_{1-40}$ in 8- and >12-month-old Tg2576 and Tg2576/SOD-2 mice. Significance was assessed with a Student's *t* test with *, $P < 0.05$.

A scatter plot illustrating this point is included in Fig. S6. All together, these findings suggest that removal of mitochondrial superoxide by overexpression of SOD-2 results in a less amyloidogenic composition of Aβ.

Discussion

Herein we have shown that reducing mitochondrial superoxide by SOD-2 overexpression prevents associative and spatial memory deficits displayed by Tg2576 mice. The reduction of mitochondrial superoxide also resulted in decreased $A\beta_{1-42}$-to-$A\beta_{1-40}$ ratio, indicative of an Aβ pool less favorable for aggregation, which is supported by our histology data showing reduced Aβ plaque deposition. It was shown previously that SOD-2 is exclusively localized to the mitochondria in the brains of SOD-2 transgenic mice (27). Because SOD-2 is localized to mitochondria and scavenges superoxide, we interpret our data as direct, in vivo evidence that mitochondrial-derived oxidative stress plays a critical role in AD pathology. The effect of mitochondrial ROS occurs downstream of early increases in Aβ but precedes plaque formation, indicating a possible involvement of mitochondrial ROS in Aβ processing during AD. Our findings are in agreement with studies linking AD to mitochondrial dysfunction (reviewed in ref. 28), including three studies that directly link SOD-2 deficiency and mitochondrial oxidative stress with increased AD pathology (13, 29, 30), and a recent study demonstrating that the mitochondrial permeability transition pore, specifically the cyclophilin D component, was involved in learning and memory deficits observed in another AD mouse model (31). Interestingly, the authors of the latter study showed that cyclophilin-D-deficient mice exhibited reduced mitochondrial ROS levels that correlated with improved cognition (31). Although it is possible that the overexpression of APP could alter the subcellular distribution of SOD-2, together with the aforementioned studies, our findings suggest that SOD-2

improves cognitive function in the Tg2576 by scavenging mitochondrial ROS.

How mitochondrial superoxide affects Aβ processing remains unknown. Changes in redox status could affect the assembly of fibrillar Aβ into plaques, thus reducing plaque load without affecting the total levels of fibrillar Aβ, as we have observed (Fig. 4 *A* and *B*). This type of dissociation between levels of fibrillar Aβ and plaque deposition has been observed previously in Tg2576 mice with the deletion of α-synuclein (32), which has been proposed to be neuroprotective and is increased following oxidative stress (33). How is Aβ processing affected by redox state? One possibility is that mitochondrial superoxide affects γ-secretase, which is responsible for cleaving APP into Aβ of different lengths (34). Recently it was proposed that the α-helical structure of the APP transmembrane domain dictates the cleavage site for γ-secretase, thereby determining which Aβ species is generated (35). Furthermore, oxidative stress has been shown to affect both the γ- and β-secretases, thereby increasing APP processing into Aβ (36). In line with these findings, our data suggest that mitochondrial superoxide could cause a conformational change in γ-secretase, altering the position of the catalytic site that causes increased efficiency of cleavage at $A\beta_{1-42}$. Consistent with this idea, mutations in presenilin 1 (the catalytic subunit of γ-secretase) have been shown to cause a preferential cleavage at $A\beta_{1-42}$ rather than the less-amyloidogenic $A\beta_{1-40}$ (34).

Oxidative stress can be detected in early as well as late AD, in both humans and animal models of AD (reviewed in refs. 37 and 38). Moreover, antioxidants have been used as a therapeutic approach to treat AD (39, 40), but have been only mildly effective, perhaps because they are not sufficiently robust or because of their nonspecific nature or incorrect timing of administration. Our studies show that a mitochondria-targeted antioxidant such as a SOD-2 mimetic could offer potentially better therapeutic outcomes in the treatment of AD. One important consideration to keep in mind is the length of antioxidant treatment. Our studies explored the therapeutic effectiveness of SOD-2 from a genetic standpoint and hence, at this stage, do not offer any insight for temporal effectiveness. Others have shown a stronger oxidant effect of Aβ on mature neurons (41), whereas another group showed a specific effect of Aβ on developing neurons and suggested beginning antioxidant therapy at 1 year of age (42). Although the timing of externally applied antioxidant therapy has yet to be clarified, our data provides strong evidence that mitochondrial-derived superoxide is an excellent target candidate for antioxidant drug development to treat AD.

Materials and Methods

Transgenic Mouse Lines. The construction of the Tg2576 transgenic mice carrying the Swedish mutant human amyloid precursor protein and the SOD-2 transgenic mice overexpressing the mitochondrial superoxide dismutase have been previously described (43, 44). Briefly, the Tg2576 mice overexpress the human APP gene carrying the Swedish mutation (K670N:M671L) under the hamster prion protein promoter and represent a mouse model for AD. The SOD-2 mice overexpress the human mitochondrial SOD under the β-actin promoter. For the purposes of this study, a male Tg2576 mouse was crossed with a female SOD-2 transgenic mouse that resulted in a progeny of WT, SOD-2, Tg2576, and Tg2576/SOD-2 mice. Experiments were performed at 4, 8, and 12–16 months of age, as noted. Genotypes were determined by using tail DNA by PCR with the following primers: 5′-CTG-ACC-ACT-CGA-CCA-GGT-TCT-GGG-T-3′ and 5′-GTG-GAT-AAC-CCC-TCCCCC-AGC-CTA-GAC-CA-3′ for APP; and 5′-CAC-AAG-CAC-AGC-CTC-CCA-G-3′ and 5′-CGC-GTT-AAT-GTG-TGG-CTC-C-3′ for SOD-2. All mice were housed at Baylor College of Medicine's transgenic mouse facility in compliance with the National Institutes of Health guidelines for Care and Use of Laboratory Animals. The mouse facility is kept on a 12-h light–dark cycle, with a regular feeding and cage-cleaning schedule.

Brain Sample Preparation. APP and SOD-2 expression in the transgenic mice was confirmed by Western blotting. $A\beta_{1-40}$ and $A\beta_{1-42}$ levels were measured by sandwich ELISA (Signet). Briefly, the left hemispheres of the brains were dissected fresh on ice and homogenized in Tris-buffered saline containing protease and phosphatase inhibitor cocktails (Sigma–Aldrich) with a glass dounce homogenizer (right hemispheres were fixed and used for histological studies). The brain homogenates were then centrifuged at 15,000 × *g* for 30 min at 4 °C, and supernatants were collected and used for Western blot analysis of APP and SOD-2 and ELISA of soluble $A\beta_{1-40}$ and $A\beta_{1-42}$. The residual pellet with insoluble Aβ species was lysed by sonication in 2% SDS followed by extraction in 70% formic acid and centrifugation. ELISA analysis of the insoluble Aβ species (both 1–40 and 1–42) was performed on the obtained supernatants.

Immunoblotting. Total proteins from brain samples were measured with a Bradford assay (Bio-Rad), and equally loaded and separated by SDS/PAGE. Proteins were then transferred onto a nitrocellulose membrane and probed with an anti-APP antibody (6E10, Signet), an anti-SOD-2 antibody (Upstate), and an anti-β-actin antibody (Sigma). This initial incubation was then followed by a horseradish peroxidase-conjugated secondary antibody (Promega) against rabbit IgG (for SOD-2) and against mouse IgG (for APP and β-actin).

Enzyme-Linked Immunosorbent Assay (ELISA). $A\beta_{1-40}$ and $A\beta_{1-42}$ were detected in mouse brain samples by sandwich ELISA using a ready kit (Signet). Both the SDS-soluble fraction (containing soluble Aβ species) and the SDS-insoluble fraction (formic acid-soluble, containing the insoluble Aβ species) were tested. Total protein concentration was measured with a Bradford assay before the ELISA and samples of equal total protein concentration were tested.

In Vivo Detection of Superoxide Using Dihydroethidium. DHE was obtained from Molecular Probes. To identify superoxide formation in the brain, DHE was used as previously described (16). Briefly, DHE-injected animals were cardiac-perfused with 4% paraformaldehyde, their were brains sectioned on a cryostat, and then sections were mounted with Vectashield H1200 containing DAPI (Vector Laboratories). Slices were evaluated for ethidium fluorescence (Ex λ = 488 nm, Em $\lambda > 590$ nm) and DAPI (Ex λ = 405 nm, Em λ = 420–480 nm) with a Zeiss LSM 10 confocal microscope. Ethidium fluorescence (indicative of superoxide levels) was quantified (by an observer blind to the genotype of the mice) in hippocampal area CA1 with the National Institutes of Health software ImageJ by using 1/4-inch squares throughout the soma of CA1 pyramidal cells, and then normalized to DAPI intensity. At least 5 sections were quantified per animal. Sections were randomly selected from the area spanning the depth of the hippocampal formation.

Amyloid Plaque Quantification. The right brain hemispheres of the same mice that were used for Western blotting and ELISA were postfixed in 4% paraformaldhehyde and then sectioned on a cryostat. Sections were stained with 1% thioflavine S in PBS for 10 min in the dark. Fluorescence was visualized following decolorizing with 95% ethanol on a Zeiss LSM 510 Meta microscope. For unbiased counting, in each animal we included all brain sections encompassing the hippocampus. Plaques were counted (by an observer blind to the genotypes of the mice) from the total surface of the section, including both cortical and hippocampal regions.

Behavioral Testing. For all behavioral experiments, at every age examined, four different groups were compared: WT, SOD-2, Tg2576, and Tg2576/SOD-2. Transgenic mice were always compared with their littermate controls, and final data were pooled to achieve an *n* of at least 8 per group. In all experiments, the experimenter was blind to the genotypes of the mice.

Locomotor activity was measured by the open field test. Briefly, mice were allowed to explore a 40 × 40 × 30-cm arena for 30 min under incandescent light and white-noise background. Activity was quantified by a computer-assisted digiscan animal activity monitor (Omnitech electronics). The parameters measured were the total distance traveled and movement time (indicators of locomotor activity), vertical activity (rearing behavior), and the center to total distance ratio (anxiety index).

Motor coordination and balance were measured by using an accelerating rotarod (UGO Basile instruments). This test consisted of placing the mice on a rotating drum and recording the time they were able to maintain their balance walking on the rotating rod. The speed of the rod accelerated from 4 to 40 rpm over 5 min. Mice were given 4 trials per day for 3 consecutive days, with 30 min inter-trial intervals. All mice used weighed similar to each other to eliminate the effect of weight on balance performance.

Sensorimotor gating was measured by testing the startle response of the mice and the prepulse inhibition (PPI) of the startle response. Briefly, the test consisted of placing the mouse in a Plexiglas cylinder connected to a startle detector. The mouse was allowed to habituate to the background 70 dB noise, and then was presented with a series of different acoustic prepulses (0, 74, 78, and 82 dB) followed by the acoustic startle stimulus. The maximum startle

amplitude was recorded and PPI was calculated as follows: %PPI = 100 − [(startle on prepulse + stimulus)/startle alone × 100].

Spatial learning and memory was tested by using the Morris water maze. During the acquisition phase, mice were given 2 blocks of 4 trials per day (60 s maximum with 1-h inter-block interval) for 4 consecutive days. A probe trial was given at the end of the last training day to determine the type of search strategy developed by the mice. The number of platform location crossings and the time spent in each quadrant was recorded in the probe trial. The numbers of target platform crossings (as percent of all platform crossings) and the time spent in the target quadrant (as percent of 60 s) were reported. On day 5, a visible platform test was administered. This task consisted of four trials (with an intertrial interval of 20 min) with the platform marked by a visible cue and moved randomly between two different locations. The visible platform escape latency was reported. The animals' trajectories were recorded with a video tracking system (Noldus EthoVision system).

Associative memory was tested by using a fear-conditioning paradigm in which the mouse was trained to associate a foot shock with a tone. The training consisted of a 2-min exploration followed by a 30-s tone (90 db white noise) at the end of which a 2-s foot shock was given (0.75 mA). The sequence of exploration, noise, and shock was repeated a second time for a total training session time of 5 min. Contextual tests (5 min total duration) were performed in the same chamber at 1–24-h after training. Cued tests were performed in a distinct chamber at 2–25-h after training for a total duration of 6 min: 3 min baseline freezing and 3 min with the tone (90 db white noise).

Data Analysis. All data are presented as mean ± SEM. Statistical analyses between two groups were performed by using a two-tailed student's *t* test, whereas comparisons involving time courses or multiple groups were performed with a two-way ANOVA followed by Tukey's post test for multiple comparisons. *P* values equal to or lower than 0.05 were considered statistically significant. Outliers were detected by applying Grubbs' method with $\alpha = 0.05$ to each experimental group (GraphPad software).

ACKNOWLEDGMENTS. We thank H. Zheng (Baylor College of Medicine, Houston) for the generous gift of the founding Tg2576 male mice, C. Spencer and R. Paylor of the Baylor College of Medicine Behavior Core facility, and all members of the Pautler and Klann labs for helpful comments. This work was supported by National Institutes of Health, National Institute of Neurological Disorders and Stroke Grants NS034007 and NS047384, and Alzheimer's Association Investigator Initiated Research Grant 05-15221 (to E.K.); National Institutes of Health, National Heart, Lung and Blood Institute Grant T32 HL07676 and American Health Assistance Foundation Grant A2008-600 (to C.A.M.); and National Institutes of Health, National Institute on Aging Grant AG029977 and The Wendler Research Fund (to R.G.P).

1. Tanzi R, Bertram L (2005) Twenty years of the Alzheimer's disease amyloid hypothesis: A genetic perspective. *Cell* 120:545–555.
2. Yankner B, et al. (1989) Neurotoxicity of a fragment of the amyloid precursor associated with Alzheimer's disease. *Science* 245:417–420.
3. Butterfield D, Griffin S, Munch G, Pasinetti G (2002) Amyloid beta-peptide and amyloid pathology are central to the oxidative stress and inflammatory cascades under which Alzheimer's disease brain exists. *J Alzheimers Dis* 4:193–201.
4. Behl C, Davis J, Lesley R, Schubert D (1994) Hydrogen peroxide mediates amyloid beta protein toxicity. *Cell* 77:817–827.
5. Tamagno E, et al. (2005) Beta-site APP cleaving enzyme up-regulation induced by 4-hydroxynonenal is mediated by stress-activated protein kinases pathways. *J Neurochem* 92:628–636.
6. Engelhart M, et al. (2002) Dietary intake of antioxidants and risk of Alzheimer disease. *JAMA* 287:3223–3229.
7. Luchsinger J, Tang M, Shea S, Mayeux R (2003) Antioxidant vitamin intake and risk of Alzheimer disease. *Arch Neurol* 60:203–208.
8. Zhu X, et al. (2005) Oxidative imbalance in Alzheimer's disease. *Mol Neurobiol* 31:205–217.
9. Reddy P, Beal M (2005) Are mitochondria critical in the pathogenesis of Alzheimer's disease? *Brain Res Brain Res Rev* 49:618–632.
10. Manczak M, Park B, Jung Y, Reddy P (2004) Differential expression of oxidative phosphorylation genes in patients with Alzheimer's disease: Implications for early mitochondrial dysfunction and oxidative damage. *Neuromolecular Med* 5:147–162.
11. Anandatheerthavarada H, Biswas G, Robin M, Avadhani N (2003) Mitochondrial targeting and a novel transmembrane arrest of Alzheimer's amyloid precursor protein impairs mitochondrial function in neuronal cells. *J Cell Biol* 161:41–54.
12. Anantharaman M, et al. (2006) Beta-amyloid mediated nitration of manganese superoxide dismutase: Implication for oxidative stress in a APPNLH/NLH X PS-1P264L/P264L double knock-in mouse model of Alzheimer's disease. *Am J Pathol* 168:1608–1618.
13. Li F, et al. (2004) Increased plaque burden in brains of APP mutant MnSOD heterozygous knockout mice. *J Neurochem* 89:1308–1312.
14. Marcus D, Strafaci J, Freedman M (2006) Differential neuronal expression of manganese superoxide dismutase in Alzheimer's disease. *Med Sci Monit* 12:BR8–14.
15. West M, Kawas C, Martin L, Troncoso J (2000) The CA1 region of the human hippocampus is a hot spot in Alzheimer's disease. *Ann NY Acad Sci* 908:255–259.
16. Hu D, Serrano F, Oury T, Klann E (2006) Aging-dependent alterations in synaptic plasticity and memory in mice that overexpress extracellular superoxide dismutase. *J Neurosci* 26:3933–3941.
17. Hu D, et al. (2007) Hippocampal long-term potentiation, memory, and longevity in mice that overexpress mitochondrial superoxide dismutase. *Neurobiol Learn Mem* 87:372–384
18. Arendash G, et al. (2001) Progressive, age-related behavioral impairments in transgenic mice carrying both mutant amyloid precursor protein and presenilin-1 transgenes. *Brain Res* 891:42–53.
19. King D, et al. (1999) Progressive and gender-dependent cognitive impairment in the APP(SW) transgenic mouse model for Alzheimer's disease. *Behav Brain Res* 103:145–162.
20. Dumont M, Strazielle C, Staufenbiel M, Lalonde R (2004) Spatial learning and exploration of environmental stimuli in 24-month-old female APP23 transgenic mice with the Swedish mutation. *Brain Res* 1024:113–121.
21. Tremml P, Lipp H, Muller U, Wolfer D (2002) Enriched early experiences of mice underexpressing the beta-amyloid precursor protein restore spatial learning capabilities but not normal openfield behavior of adult animals. *Genes Brain Behav* 1:230–241.
22. Westerman M, et al. (2002) The relationship between Abeta and memory in the Tg2576 mouse model of Alzheimer's disease. *J Neurosci* 22:1858–1867.
23. Barnes P, Good M (2005) Impaired Pavlovian cued fear conditioning in Tg2576 mice expressing a human mutant amyloid precursor protein gene. *Behav Brain Res* 157:107–117.
24. Kawarabayashi, T et al. (2001) Age-dependent changes in brain, CSF, and plasma amyloid (beta) protein in the Tg2576 transgenic mouse model of Alzheimer's disease. *J Neurosci* 21:372–381.
25. Roychaudhuri R, Yang M, Hoshi M, Teplow D (2008) Amyloid beta-protein assembly and Alzheimer's disease. *J Biol Chem* 284:4749–4753.
26. Hansson O, et al. (2007) Prediction of Alzheimer's disease using the CSF Abeta42/Abeta40 ratio in patients with mild cognitive impairment. *Dement Geriatr Cogn Disord* 23:316–320.
27. Maragos W, et al. (2000) Methamphetamine toxicity is attenuated in mice that overexpress human manganese superoxide dismutase. *Brain Res* 878:218–222.
28. Wang X, Su B, Perry G, Smith M, Zhu X (2007) Insights into amyloid-beta-induced mitochondrial dysfunction in Alzheimer disease. *Free Radic Biol Med* 43:1569–1573.
29. Esposito L, et al. (2006) Reduction in mitochondrial superoxide dismutase modulates Alzheimer's disease-like pathology and accelerates the onset of behavioral changes in human amyloid precursor protein transgenic mice. *J Neurosci* 26:5167–5179.
30. Melov S, et al. (2007) Mitochondrial oxidative stress causes hyperphosphorylation of tau. *PLoSONE* 2:e536.
31. Du H, et al. (2008) Cyclophilin D deficiency attenuates mitochondrial and neuronal perturbation and ameliorates learning and memory in Alzheimer's disease. *Nat Med* 14:1097–1105.
32. Kallhoff V, Peethumnongsin E, Zheng H (2007) Lack of alpha-synuclein increases amyloid plaque accumulation in a transgenic mouse model of Alzheimer's disease. *Mol Neurodegener* 2:6.
33. Quilty MC, et al. (2006) Alpha-synuclein is upregulated in neurones in response to chronic oxidative stress and is associated with neuroprotection. *Exp Neurol* 199:249–256.
34. Xia W, et al. (1998) Presenilin 1 regulates the processing of beta-amyloid precursor protein C-terminal fragments and the generation of amyloid beta-protein in endoplasmic reticulum and Golgi. *Biochemistry* 37:16465–16471.
35. Tan J, et al. (2008) Effects of gamma-secretase cleavage-region mutations on APP processing and Abeta formation: Interpretation with sequential cleavage and alpha-helical model. *J Neurochem* 107:722–733.
36. Tamagno E, et al. (2008) Oxidative stress activates a positive feedback between the gamma- and beta-secretase cleavages of the beta-amyloid precursor protein. *J Neurochem* 104:683–695.
37. Su B, et al. (2008) Oxidative stress signaling in Alzheimer's disease. *Curr Alzheimer Res* 5:525–532.
38. Pratico D (2008) Oxidative stress hypothesis in Alzheimer's disease: A reappraisal. *Trends Pharmacol Sci* 29:609–615.
39. Quinn J, et al. (2007) Chronic dietary alpha-lipoic acid reduces deficits in hippocampal memory of aged Tg2576 mice. *Neurobiol Aging* 28:213–225.
40. Ju T, Chen S, Liu C, Yang D (2005) Protective effects of S-nitrosoglutathione against amyloid beta-peptide neurotoxicity. *Free Radic Biol Med* 38:938–949.
41. Liu T, et al. (2004) Amyloid-beta-induced toxicity of primary neurons is dependent upon differentiation-associated increases in tau and cyclin-dependent kinase 5 expression. *J Neurochem* 88:554–563.
42. Sompol P, et al. (2008) A neuronal model of Alzheimer's disease: An insight into the mechanisms of oxidative stress-mediated mitochondrial injury. *Neuroscience* 153:120–130.
43. Hsiao K, et al. (1996) Correlative memory deficits, Abeta elevation, and amyloid plaques in transgenic mice. *Science* 274:99–102.
44. Ho Y, Vincent R, Dey M, Slot J, Crapo J (1998) Transgenic models for the study of lung antioxidant defense: Enhanced manganese-containing superoxide dismutase activity gives partial protection to B6C3 hybrid mice exposed to hyperoxia. *Am J Respir Cell Mol Biol* 18:538–547.